Zeolitic diagenesis of Oligocene pyroclastic rocks of the Metaxades area, Thrace, Greece

P. TSOLIS-KATAGAS AND C. KATAGAS

Department of Geology, University of Patras, 261 10 Patras, Greece

Abstract

The unstable glassy component of the Oligocene tuffaceous sediments of the Metaxades area, Thrace, Greece, has undergone extensive zeolitic diagenetic alteration. The authigenic minerals occur as crypto- to micro-crystalline aggregates making up most of the matrix in the altered tuffs and as precipitates in cavities produced by dissolved glass fragments. Glass-shard pseudomorphs are ubiquitous and most of them are partly filled by one or more of the minerals smectite, heulandite, mordenite and silica.

The heulandite group zeolites are mostly high-silica calcium-rich heulandites showing intermediate thermal behaviour between most heulandites and clinoptilolites. Their Si/Al ratios are similar to clinoptilolite (4.74–5.19) but their divalent/monovalent cation ratios (1.5–3.24) are partly superposed onto the ratios of heulandite group 1 and 2 and differ considerably from the values of the relevant ratio in clinoptilolite. Rare K-rich clinoptilolite crystals have been identified in one sample only.

Based on field observations, compositions and paragenetic relationships of coexisting authigenic minerals and the absence of critical phases such as laumontite, analcime or authigenic albite, it is suggested that the Metaxades pyroclastic rocks underwent burial diagenesis intermediate between Iijima's (1978) zones II and III commonly developed in silica saturated environments.

KEYWORDS: heulandite, clinoptilolite, mordenite, burial diagenesis, zeolite, Thrace, Greece.

Introduction

ZEOLITE-BEARING mineral assemblages in pyroclastic deposits of marine Tertiary basins are widespread in the area of Eastern Rhodope, Bulgaria (Aleksiev and Djourova, 1975); their formation has been attributed by the above authors to the so-called 'geo-autoclave' type. Zeolite diagenesis is also of particular interest in western Thrace, Greece, because of the abundance of volcanogenic sediments in the Tertiary geologic record of the area (cf. Fytikas *et al.*, 1984). Acid pyroclastic deposits occur in the Metaxades area, near the Greek–Bulgarian border; this deposit has been quarried for local building purposes and only very recently gained the attention of investigators interested in zeolitization. Clinoptilolite, clay minerals and cristobalite were recognized in the Metaxades deposit by Marantos *et al.* (1988) and Tsirambides *et al.* (1988). However, heulandite and mordenite had not been previously recognized in this deposit. During the past few years the minerals of the heulandite group have been the subject of numerous studies, which have improved our knowledge on their crystallochemical parameters. Our investigation concentrated mainly on the crystal chemistry of the heulandite-group zeolites and the diagenetic history of the pyroclastic deposit of Metaxades.

Geological setting

Zeolitic alteration products of acid pyroclastics outcrop in the Metaxades area, at the southern part of the Tertiary Orestias basin (Fig. 1). The latter, started during the lower Lutetian on the metamorphic formations of the Rhodope Massif and the Circum Rhodope unit, with coarse conglomerates grading upwards into a sequence of interbedded siltstone, sandstone and clay layers. The pyroclastics overlay a middle to Upper Eocene 40–50 m thick limestone (Andronopoulos, 1977). Marine microfossils found in a limestone bed at the upper parts of the pyroclastics suggest a lower Oligocene age (Marantos *et al.*, 1988). Radiometric dates show also that volcanic activity in the Greek part of Thrace developed from 33 to 23.6 Ma (Fytikas *et al.*, 1984). The thickness of the pyroclastics in the studied area is about 35 m; the rocks at the base differ from

Mineralogical Magazine, March 1990, Vol. 54, pp. 95–103

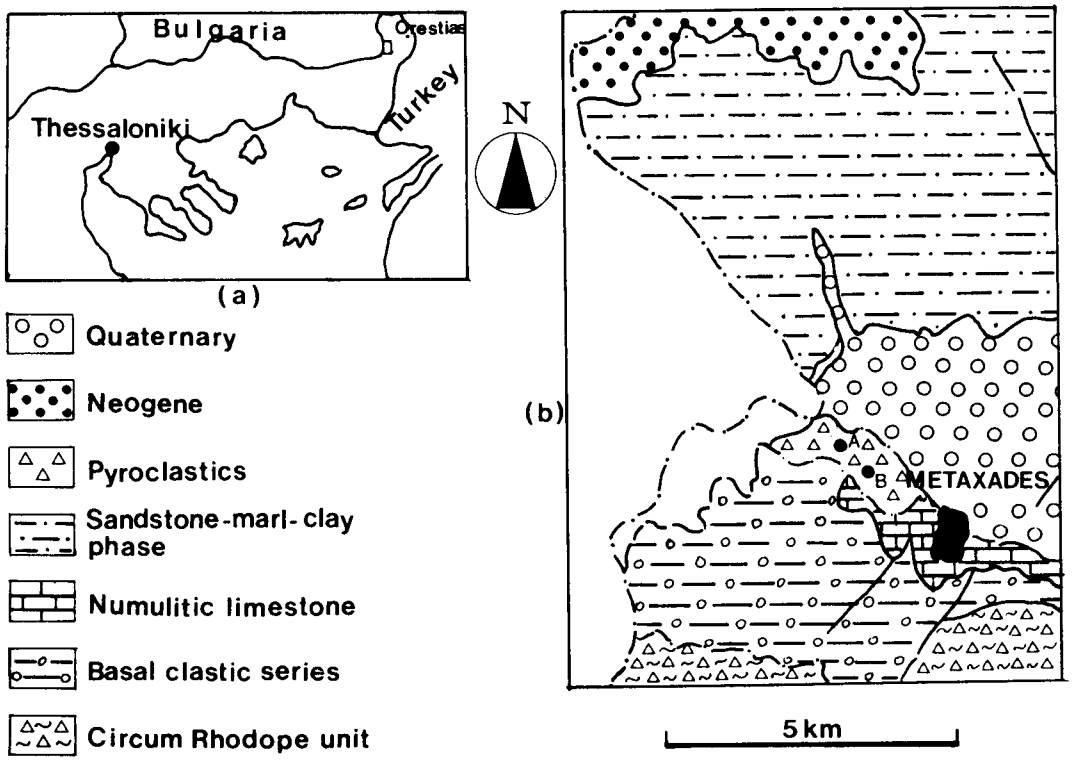

FIG. 1. (*a*) Location of Metaxades area. (*b*) Simplified geological map of the Metaxades area (after N. Solakious and P. Papadopoulos, 1988) showing the sampling locations for the stratigraphic sections A (samples 1–15) and B (samples 16–32).

those stratigraphically above in both primary and authigenic mineralogy and texture. The basal bed is a coarse sandstone with poorly to moderately sorted angular to subangular extra-formational fragments of feldspar, muscovite, biotite, hornblende, epidote, garnet and metamorphic rocks cemented by calcite; it grades upwards inversely into a conglomerate consisting of subangular to subrounded pebbles of metamorphic rocks cemented by vitric and crystal light green coloured, ash size, welded pyroclastics. The maximum clast size in the conglomerate is *c.* 10mm. The whole sequence above the conglomerate consists mainly of zeolitized vitric and crystal tuffs mixed with epiclastic grains derived from pre-existing rocks and is characterized by multiple graded bedding. The tuffs are white to pale grey, yellow or green in colour, thinly to medium bedded and locally thinly to thickly cross-laminated. There exists an overall decrease in grain size upwards as can be shown mainly by the coarsest particles of the beds. Individual graded beds encountered in the middle and upper units of the section show less pronounced changes in grain size between the base and top layers than do the more basal units, and often bedding may be defined only by changes in colour or mineralogical composition. In the uppermost part of the section coarse sandstones with crystal and lithic fragments of metamorphic origin, very similar to those encountered in the basal beds, mark the end of the volcanic episode. This calcite-cemented sandstone is overlain locally by a zeolitized tuff bed (sample M15), the presence of which suggests the beginning of a new ash fall episode (cf. Lilov *et al.*, 1987). It is unclear whether the last episode was a major or minor one, as the original thickness of the pyroclastics of this cycle is unknown.

Methods of study

Sampling was carried out in two supplementary stratigraphic sections, each approximately 17m thick; their locations are shown in Fig. 1(b). Powder pack mounts were used to produce random orientation for bulk X-ray diffraction (XRD)

TABLE 1. Representative bulk rock and mineralogical compositions of altered pyroclastic and psammitic rocks from the Metaxades deposit. Samples are arranged from upper to lower stratigraphic horizons and mineral assemblages are arranged in decreasing relative abundance. (C=Cristobalite; Cc=Calcite; H=Heulandite; I-S=Illite-smectite; M=Mordenite; S=Smectite).

	M15	M13	M7	M4	M16	M21	M24	M27	M28	M32
SiO_2	70.77	65.46	71.37	73.88	71.34	71.14	67.80	73.19	70.15	45.98
Al_2O_3	11.73	10.56	9.95	9.90	10.10	9.71	11.19	9.45	10.69	9.94
Fe_2O_3	0.77	2.47	0.49	0.38	0.90	0.70	0.88	1.05	0.91	3.63
MgO	0.61	1.18	0.58	0.40	0.71	0.51	0.48	0.45	0.49	1.39
CaO	2.37	6.48	2.65	1.63	2.54	2.99	3.60	2.83	3.28	20.40
Na_2O	1.64	0.53	0.55	0.39	0.64	1.06	1.06	1.20	1.08	1.54
K_2O	2.74	4.45	2.79	4.80	3.17	2.89	3.21	2.46	2.88	1.46
TiO_2	0.10	0.32	0.10	0.08	0.13	0.11	0.11	0.14	0.13	0.39
P_2O_5	0.02	0.05	0.01	0.01	0.02	0.02	0.02	0.02	0.02	0.08
MnO	0.01	0.06	0.01	0.02	0.02	0.04	0.08	0.10	0.07	0.28
H_2O^-	3.56	1.00	4.15	2.69	3.38	3.48	3.90	3.25	3.42	0.50
L.O.I.	5.24	6.84	6.90	4.92	6.21	6.87	7.06	5.19	6.44	13.66
Total	99.56	99.40	99.55	99.10	99.16	99.52	99.39	99.33	99.56	99.25
	H,C,M	I-S,Cc	H,M,C,S	H,C,M,S	H,M,S	H,M,C,S	H,C,M	H,M,C,S	H,M,C,S	Cc,I-S

mineral analyses. For each sample three mounts were prepared and investigated after heating at 260, 400 and 550°C to determine whether intensity reduction of the (020) and other X-ray reflections of the heulandite-group zeolites occurred. For clay mineral identification the $<2\,\mu m$ size fractions were obtained and oriented mounts were prepared on glass slides. The mounts were run using a Philips diffractometer and Ni-filtered Cu-$K\alpha$ radiation. Glycerol treatment and heating at 490°C for 2 hr aided their identification. Relative abundances of authigenic minerals were estimated from the powder diffractometer patterns by using peak intensities. Chemical analyses of the bulk samples were carried out using the Li tetraborate fusion method for Si and Ti and ICP on $HF/HClO_4$ solutions for the rest of the elements. Selected samples were examined in thin section and by scanning electron microscopy (SEM) using a JEOL JSM 820 instrument. Mineral compositions were determined with a Link system energy-dispersive X-ray analyser attached to a Cambridge Geoscan microprobe. Live time of 100 seconds and an acceleration voltage of 20 kV were the general analytical conditions. The quality of the analyses was calculated by spot checking the charge balance error,

$$E=\frac{(Al+Fe)-(Na+K)-2(Mg+Ca)}{(Na+K)+2(Mg+Ca)}\times 100.$$

Petrography and authigenic mineralogy

The mineralogical composition of representative altered pyroclastics as determined by microscopic observation and XRD analysis is given in Table 1. It is evident from this table that the pyroclastic pile is sandwiched between two sandstone beds characterized by similar authigenic and detrital mineralogy. Authigenic minerals in these 30–40 cm thick beds include abundant smectite, a mixed-layer illite-smectite and calcite (sample M32 at the base and M13 at the top of the pile).

Microscopic observation suggests that the original texture of the zeolite-bearing rocks was either pyroclastic or epiclastic with a high percentage of glass in the matrix. Throughout the tuffaceous sediments it is mainly the unstable glassy component that has undergone extensive diagenetic alteration; the primary crystals are generally fresh and only in few specimens, K-feldspar grains have slightly diffuse boundaries produced by incipient solution. The degree of alteration seems to be primarily related to sorting and grain size. Layers with much fine material are more altered than the coarser, better sorted layers. The authigenic minerals occur *(a)* as crypto- or microcrystalline aggregates making up most of the matrix in the altered tuffs and *(b)* as precipitates in cavities and partly or wholly filled veinlets, produced by dissolved glass fragments. Glass shard pseudomorphs are ubiquitous in the examined

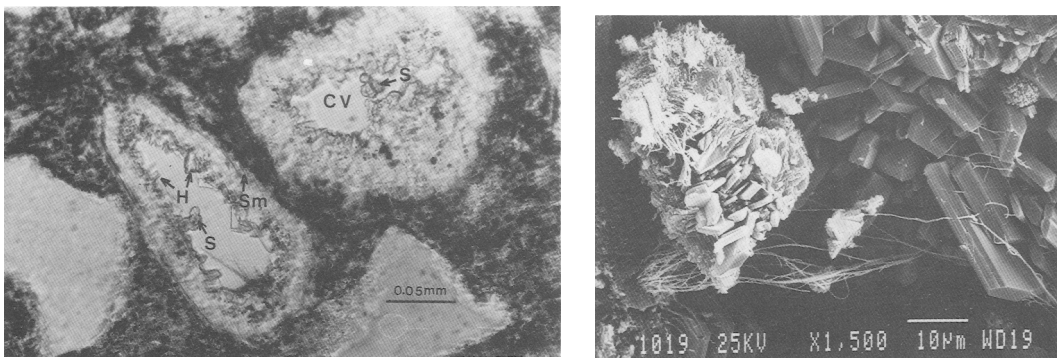

FIG. 2 (*left*). Photomicrograph illustrating modes of occurrence of zeolites and associated authigenic minerals in glass shard pseudomorphs in sample M7 (H = heulandite, S = silica, Sm = smectite, CV = central cavity). Mordenite, although present, is too fine to be recognized with the optical microscope. FIG. 3 (*right*). Scanning electron micrograph of sample M21 showing platy clinoptilolite, filiform mordenite that criss-cross between clinoptilolite plates, and aggregates of closely packed cristobalite crystallites. Radiating mordenite fibres in lower left corner of the micrograph apparently replaced the rim of glass.

specimens. Most of the pseudomorphs are partly filled by one or more of the minerals smectite, heulandite, mordenite and silica (Fig. 2). Smectite commonly forms thin linings coating the edges of the pseudomorphs surrounding one or two more internal zeolite-rich layers: a layer of cryptocrystalline randomly oriented heulandite and/or a layer of finely crystalline tabular grains of heulandite aligned perpendicular to the glass shard pseudomorph wall and globular opal within the cavity. Some pseudomorphs, especially in the more fine grain size samples are entirely filled by randomly oriented anhedral to euhedral coarser zeolite grains or by radiating crystals of the same mineral with or without co-precipitated cristobalite.

Heulandite-group zeolites

Heulandite is the predominant zeolite in the Metaxades volcaniclastics but varies in abundance from traces in sandstones up to about 50% in altered vitric tuffs. In the $<2\,\mu m$ fraction, oriented samples prepared for the XRD analysis of clay minerals, the (020) reflection of heulandite was enhanced due to either preferred orientation of its microcrystals caused by the perfect cleavage along (010) or because heulandite is most abundant in the $<2\,\mu m$ fraction (cf. Petrov *et al.*, 1984). Scanning electron micrographs show that heulandite crystals display tabular or coffin-shaped morphology lining or filling cavities of dissolved glass shards (Fig. 3). Heulandite crystals are usually grown with their long axis perpendicular to shard margins and sometimes crystals showing ragged morphology may coexist with euhedral crystals (Figs. 2, 3).

No heulandite has been previously recognized in these pyroclastics; instead clinoptilolite was referred to as their predominant zeolite constituent by previous workers (Marantos *et al.*, 1988; Tsirambides *et al.*, 1988). Heat treatment techniques proposed by Mumpton (1960), Alietti (1972) and Boles (1972) and, where grain size permitted, electron probe analyses were used to distinguish between heulandite and clinoptilolite. The heat treatment of the studied samples at 260°C for two hours and at 400°C overnight did not result in the appearance of a polymorphic phase. However the latter heating did result in 80–90% intensity reduction of the basal peak reflection and further overnight heating at 550°C verified structural collapse (Fig. 4). Destruction of the lattice at such temperature conditions characterizes heulandite of group 2, whereas the absence of no contracted phases after heating characterizes heulandite of group 3 (clinoptilolite) (cf. Alietti, 1972; Boles, 1972). Electron probe analyses of heulandite-group zeolites from sample M23 revealed that Ca-rich heulandite coexists with rare K-rich clinoptilolite (Table 2); it is therefore suggested that such intermediate thermal properties could not be easily attributed to the heulandite–clinoptilolite mixtures (cf. Shepard, 1961; Ratterman and Surdam, 1981). Representative electron microprobe analyses of single crystals of the heulandite-group zeolites, recalculated on the basis of the 72 oxygen atoms are given in Table 2. The sum of the exchangeable cationic charges in the unit cell of the analyses is only less than 0.5 units than the number of R^{3+} cations

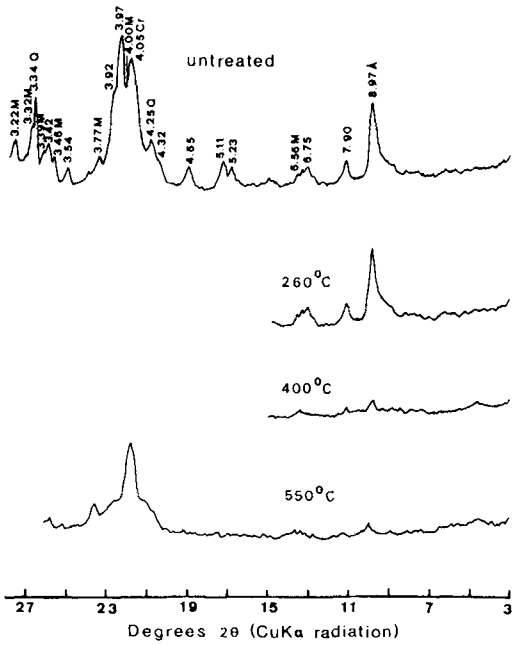

FIG. 4. X-ray powder diffractograms of untreated and heated samples. All unlabelled peaks belong to heulandite-group minerals. M = mordenite; Cr = cristobalite; Q = quartz (*d*-values are in Ångstroms) (Sample M23).

in the tetrahedral sites and the balance error *(E)* for the analyses is less than the commonly acceptable 10%. Thus, the analyses may be considered as satisfactory. The analyses presented in Table 2 reveal noticeable differences not only between heulandite crystals encountered in different samples but also between crystals in the same sample. Calcium exceeds alkalis (52–75% of the exchangeable cations) and potassium predominates over sodium in all but one analyses (M23–8). Despite the extensive variation in composition among crystals of the same sample, a slight variation in the heulandite composition with depth is observed; heulandite from the lower horizons (e.g. M23, M28) is apparently less (Mg + Ca)-rich and more (Na + K)-rich than heulandite from the upper horizons of the pyroclastic pile (e.g. M4, M7).

The Si/Al ratios are 4.74–5.19 ($\overline{M} = 4.95$) and according to the classification scheme of Boles (1972) all the crystals analysed would be classified as clinoptilolite. Their divalent/monovalent cation ratios however, ranging from 1.5 to 3.24 ($\overline{M} = 1.85$) are partly superposed onto the ratios of heulandite 1 and 2 (cf. Alietti *et al.*, 1977) and differ considerably from the values given by Boles (1972) and Alietti (1972) for the relevant ratio in clinoptilolites (0.09–0.6). Gottardi and Galli (1985) based on a large set of data by Alietti *et al.* (1977) give a triangular plot $Si_{36}O_{72}$–$(Mg + Ca + Sr + Ba)_9Al_{18}Si_{18}O_{72}$–$(Na + K)_{18}Al_{18}Si_8O_{72}$ in which they attempt to separate the fields of the heulandite-group zeolites according to their thermal behaviour (Fig. 5). The dashed dotted line is the boundary where Na + K = Ca + Mg, i.e. the boundary heulandite-clinoptilolite after Mason and Sand's (1960) nomenclature of the heulandite group. The dotted line at Si : Al = 4 is the boundary between heulandite-group zeolites after Boles (1972). The compositions of the heulandite-group zeolites from Metaxades plot on either side of the dividing line of the fields of heulandite of thermal behaviour 2 and 3 and, with the exception of the clinoptilolite of sample M23 into the heulandite field, after Mason and Sand's (1960) definition. Compared to Ca-rich heulandite group zeolite compositions reported in the literature, the heulandite of the present study is similar to some heulandites of thermal behaviour 2 and Ca-rich clinoptilolites listed in Alietti *et al.* (Table 2, 1977) (Fig. 5). Note, however, that some heulandites of thermal group 2 and clinoptilolites (thermal group 3) have very similar Si/Al ratios. Ratterman and Surdam (1981) and Tsolis-Katagas and Katagas (1989) found also no significant differences between $Si/(Al + Fe^{3+})$ in different heulandite-group zeolites and from their data, this group of minerals appears to be best distinguished on the basis of their cation contents.

Mordenite

Mordenite is present in small amounts in most of the studied samples. It is commonly associated with heulandite, cristobalite and smectite (Fig. 4). SEM shows that mordenite occurs as fibrous masses commonly intertwine into mesh structures (Fig. 6) or as individual thin fibres, <0.5 μm in diameter and about 20–80 μm long, scattered over heulandite crystals or cristobalite spherules inside relict glass shard outlines (Figs. 3, 6). SEM observations on sample M21 suggest that mordenite crystals formed from and around the relict glass (Fig. 3). The fibres and masses of mordenite were too fine to be analysed by electron microprobe.

Cristobalite

Cristobalite is the authigenic silica mineral present in the studied samples. It occurs mainly in spherules or oval shaped aggregates composed of small (< 1 μm) closely crystallites, associated with heulandite and mordenite (Figs. 3, 6). Cristobalite is absent from smectite-rich samples. Quartz is ubiquitous and is considered to be detrital.

TABLE 2. Representative electron microprobe analyses of Heulandite group zeolites from the Metaxades pyroclastic rocks.

	M7-12	M7-19	M4-12	M4-20	M21-13	M21-16	M23-4	M23-7	M23-8	M28-1	M28-7
SiO_2	67.34	67.54	67.22	66.92	67.07	66.54	64.75	66.75	64.65	67.67	67.74
TiO_2	0.02	0.02	0.01	0.07	0.00	0.00	0.00	0.09	0.00	0.00	0.00
Al_2O_3	11.74	11.05	11.64	11.81	11.16	11.66	10.89	11.29	11.10	11.54	12.12
FeO	0.03	0.06	0.03	0.02	0.05	0.02	0.04	0.09	0.11	0.17	0.04
MnO	0.00	0.00	0.00	0.03	0.00	0.00	0.00	0.07	0.02	0.00	0.01
MgO	0.45	0.42	0.42	0.34	0.26	0.35	0.31	0.49	0.41	0.19	0.13
CaO	4.24	3.88	4.20	4.81	4.18	4.33	4.08	4.08	3.08	4.20	4.59
Na_2O	0.19	0.07	0.15	0.00	0.08	0.11	0.00	0.30	0.35	0.27	0.10
K_2O	2.19	2.15	1.85	1.36	2.07	2.27	2.62	2.67	4.71	2.09	2.23
Total	86.20	85.19	85.52	85.36	84.87	85.28	82.69	85.83	84.36	86.13	86.96
	unit cell content based on 72(O)										
Si	29.88	30.22	29.97	29.85	30.15	29.86	30.02	29.88	29.77	30.03	29.82
Ti	0.01	0.01	0.01	0.02	0.00	0.00	0.00	0.03	-	0.01	0.00
Al	6.14	5.83	6.11	6.21	5.91	6.17	5.95	5.96	6.10	6.03	6.29
Fe	0.01	0.02	0.01	0.01	0.02	0.01	0.02	0.04	0.02	0.06	0.01
Mn	0.00	0.00	0.00	0.01	0.00	0.00	0.00	0.03	0.01	0.00	0.00
Mg	0.30	0.28	0.28	0.23	0.17	0.24	0.22	0.33	0.28	0.13	0.09
Ca	2.01	1.86	2.01	2.30	2.01	2.08	2.03	1.96	1.52	2.00	2.16
Na	0.16	0.06	0.13	0.00	0.07	0.10	0.00	0.26	0.31	0.23	0.09
K	1.24	1.23	1.05	0.78	1.19	1.30	1.55	1.53	2.76	1.18	1.25
Si:Al	4.87	5.18	4.90	4.81	5.10	4.84	5.05	5.02	4.94	4.98	4.74
(Ca+Mg):(Na+K)	1.65	1.67	1.92	3.24	1.73	1.66	1.45	1.28	0.58	1.50	1.68
E%	+2	+4.8	+6.6	+6.7	+5.6	+2.3	-1.2	-5.6	9.6	+8.14	+7.89

Clay minerals

Smectite is the main clay mineral, present in small amounts in most of the samples. Illite and mixed-layer illite–smectite has been identified in the clay fraction of samples collected from the upper and lower horizons of the pile. X-ray powder diffraction analyses indicate that clay minerals are more abundant in the coarser fractions of the samples.

Host rock composition

The original composition of the tuff is unknown, however whole-rock analyses and compositions of pyrogenic crystals indicate that the protoliths were probably of dacite to rhyolite composition. Table 1 lists major element compositions of representative samples from the zeolitic tuffs and the upper and lower sandstone horizons. The compositions of samples from these horizons (M13 and M32 respectively) differ in most of their major element contents compared to the zeolitic samples; Ca/(K + Na) ratios are higher in the former and Si/Al ratios are higher in the latter samples. A plot of the Ca/(K + Na) in the rock versus the mean (Ca + Mg)/(K + Na) ratio of the analysed heulandite crystals in each sample reveals an antipathetic relationship suggesting that other factors, such as composition of the circulating fluids may partly control the composition of authigenic minerals.

Discussion

The complete breakdown of the Ca-rich heulandite group zeolite studied here at 550°C and the absence of contracted phases at lower temperatures support the conclusion reached by several workers that slight differences in the type of the exchangeable cations play an important role in the thermal behaviour of the heulandite-group zeolites. The anomalous intermediate' thermal behaviour of the examined Ca-rich heulandite-group phase between most heulandites and clinoptilolites may be attributed to its distinct number and kind of monovalent and divalent cations that participate in the 'zeolitic' substitution ($Na + K \rightleftharpoons Ca$) and to its high Si/Al ratio rather, than to heulandite clinoptilolite mixtures.

From the foregoing account on the compositions, paragenetic relationships of coexisting

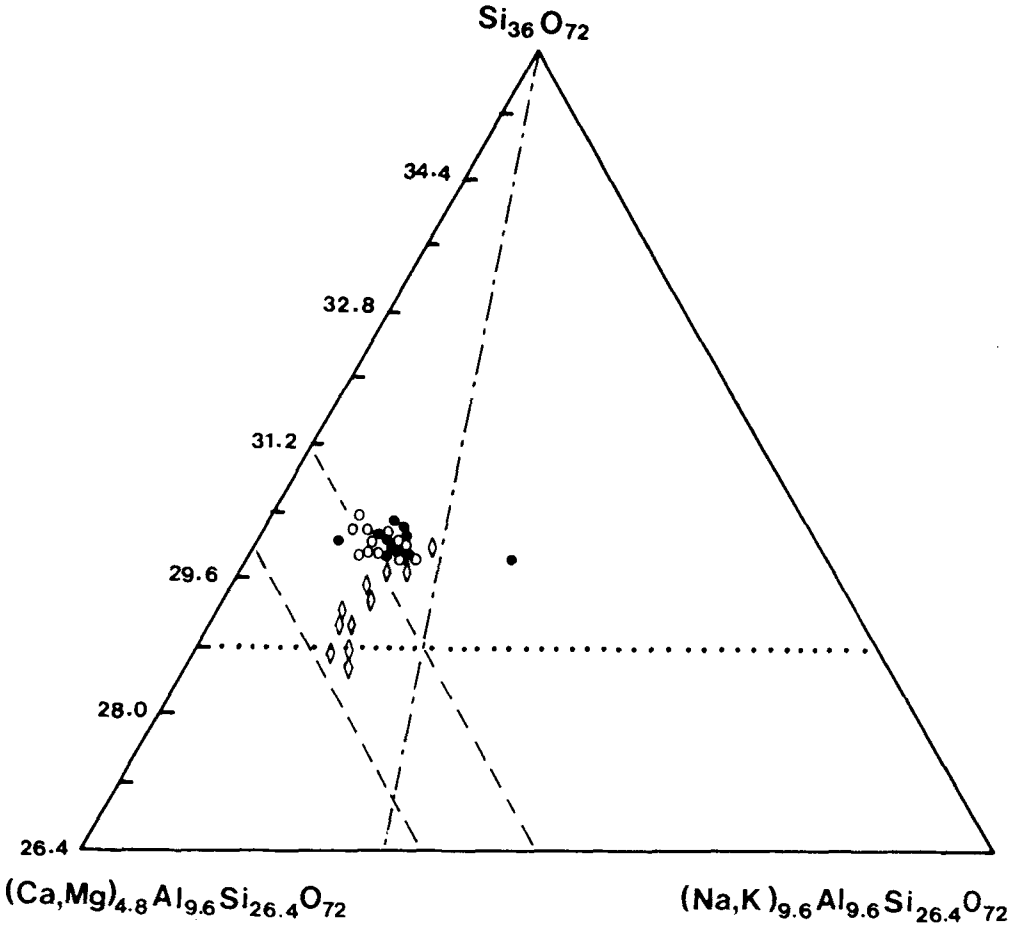

FIG. 5. Mole plot of heulandite and clinoptilolite from Metaxades. Plots include analyses in addition to those given in Table 2 (open symbols). Open diamonds represent compositions of Ca-rich heulandite-group zeolites reported in Alietti *et al.* (1977). Lines shown in the diagram are explained in the text.

authigenic phases and field observations, the possible zeolitization processes of the Metaxades pyroclastics should now be considered.

Aleksiev and Djourova (1975) proposed a 'geo-autoclave type' model for the zeolitization of the clinoptilolite-rich Oligocene marine deposit of the north-eastern Rhodope, Bulgaria. Although the Metaxades deposit is probably comparable spatially and temporally with those in Bulgaria, the presence of clastic grains of minerals and rocks from the surrounding metamorphic formations throughout the deposit, suggests that the accumulation of the pyroclastic pile was not accomplished very rapidly. Consequently, during the time span of their deposition, the pyroclastic would have probably lost much of their initial thermal energy.

The thickness of the marine Oligocene zeolitized volcaniclastic rocks, the shallow character of the underlying and overlying sedimentary strata, the lack of diagnostic authigenic minerals and modes of their occurrence characterizing marine zeolitic deposits formed by local heat sources, the extensive zeolitization and the uniform distribution of the heulandite–mordenite-bearing assemblages throughout the pyroclastic materials in Metaxades area, suggest that the authigenic silicate minerals could have resulted from a burial diagenetic alteration. Borehold data reveal that the thickness of the sediments in the basin is roughly 2750 m (J. Karfakis, Institute of Geological and Mineral exploration, Athens, personal communication, 1989) but burial depths are unknown. The burial depth of Metaxades pyroclastic was probably not greater than 1500 m (i.e.

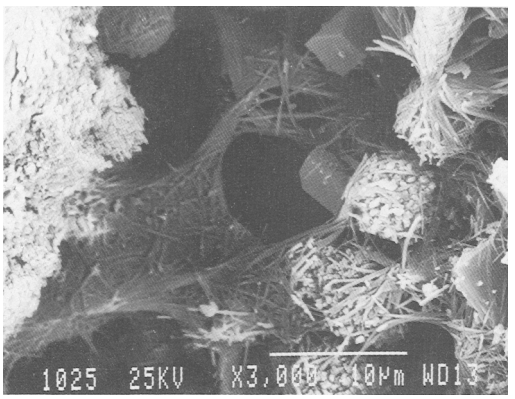

FIG. 6. Scanning electron micrograph of sample M23 showing intertwined mordenite fibres, euhedral heulandite crystals and spherules of closely packed cristobalite crystallites.

the estimated thickness of the overlying Oligocene and younger sediments) assuming that the entire stratigraphic sequence was present in the area. Such a depth of burial is shallower but comparable to that reported by Iijima (1978) for the boundary between zones II and III developed in silicic volcanic sediments in a thick column of marine deposits due to burial diagenesis (e.g. Yabase oil field, Japan). The zonal character of the burial diagenesis reported by other authors (e.g. Utada, 1970; Hay, 1966; Iijima and Utada, 1971; Iijima, 1978; Moncure *et al.*, 1981) does not emerge from the available data, probably because the proper raw material in Metaxades appears at one level only. Gottardi and Obradović (1978) list many such occurrences from various other parts of the world. Iijima (1978), in his general scheme of zeolitic crystallization in burial diagenesis, regards alkali clinoptilolite and mordenite as the most common and typical zeolites in his zone II, which is under zone I (characterized by silicic glass altered to montmorillonite and opal-CT) and above zone III. The latter is subdivided into analcime–heulandite (IIIa) and analcime–laumontite (IIIb) subzones. According to Iijima, the high-silica and alkali-rich clinoptilolite in zone II is replaced by high-silica heulandite in the upper part of zone IIIa, probably via intermediate Ca-rich clinoptilolite. High-silica–alkali-rich clinoptilolite was detected in only one sample (M23) and mordenite coexists with high-silica heulandite of group 2 in nearly all the samples. This latter phase may be considered as equivalent to the intermediate Ca-rich clinoptilolite. It is therefore suggested that the Metaxades pyroclastics underwent a burial diagenesis intermediate between Iijima's zones II and III. The absence of laumontite, analcime, authigenic albite/or albitized plagioclase as well as the presence of montmorillonite and the scarcity of the 15–14 Å mixed-layer clay suggest also that the burial conditions in the silica-saturated environment of the Metaxades deposit were insufficient to promote the reaction clinoptilolite → analcime → albite and heulandite → laumontite.

The stages of alteration of the pyroclastic material leading to the formation of the heulandite–mordenite-bearing assemblages cannot be determined due to lack of mineralogical zoning. Textural evidence suggests that in the Metaxades deposit, as elsewhere, montmorillonite was among the first minerals to crystallize as the glass dissolved; the outer walls of most of the glass-shard pseudomorphs are lined with a thin layer of clay (Fig. 2). The early formation of clay was probably favoured by a relatively low $(Na+K)/H^+$ activity ratio in the pore fluid (Hemley, 1962). The alteration of glass to smectite would have raised the pH, a_{SiO_2}, and $(Na+K)/H^+$ activity ratio, providing thus a chemical environment favourable for the formation of heulandite-group zeolites (Hay, 1966; Hay and Sheppard, 1977; Hay and Guldman, 1987). The scarcity of K-rich clinoptilolite in the studied samples suggests that either heulandite was formed from pre-existing clinoptilolite as the depth of burial and temperature increased, or that heulandite grew directly from a favourable solution. Variations in the composition of heulandite crystals shown in Table 2 may be attributed to minor variations in activities of ionic species in solution. The formation of Ca–K-rich heulandite-group zeolites may have caused an increase in the Na/K ratio in the solution. Solutions greatly enriched in Na^+ relative to K^+ apparently were unfavourable for heulandite-group zeolites and the latter became unstable with respect to the more Na-rich mordenite (Hay, 1966; Hawkins *et al.*, 1978). Physicochemical analysis of mineral parageneses in zeolitized perlites by Kanazirski and Yanev (1983), suggests that mordenite is the stable phase at lower μH_2O (higher T) and μCaO with respect to clinoptilolite. Scanning electron micrographs show the late precipitation of mordenite fibres over heulandite crystals or globular bodies of cristobalite (Figs. 3, 6); it is therefore suggested that the development of mordenite in the Metaxades deposit could have been driven by either changes in chemistry of the solutions or P/T conditions (depth of burial) or both.

Acknowledgements

We thank M. G. Audley-Charles for providing hospitality during our sabbatical at the Department of Geological Sciences, University College London, where the analytical work was carried out. We are indebted to B. Roberts for allowing us to use the equipment at the department of Geology, Birkbeck College, University of London, and to S. R. Hirons and A. D. Beard for technical assistance. Special thanks are due to P. Papadopoulos for helpful discussions in the field.

References

Aleksiev, B. and Djourova, E. G. (1975) *C.R. Acad. Bulg. Sci.* **28,** 517–20.

Alietti, A. (1972) *Am. Mineral.* **57,** 1448–62.

—— Brigatti, M. F. and Popi, L. (1977) *Neues Jahrb. Mineral., Mh.*, 493–501.

Andronopoulos, B. (1977) *Geol. Geophys. Research, Institute of Geology and Mineral Exploration, Athens,* **17,** 59 pp. (in Greek).

Boles, J. R. (1972) *Am. Mineral.* **57,** 1463–93.

Fytikas, M. Innocenti, F., Manetti, P., Mazzuoli, R., Peccerilo, A., and Villari, L. (1984). *The Geological Evolution of the Eastern Mediterranean* (J. E. Dixon and A. H. F. Robertson, eds.) Geol. Soc. Sp. Publication No. 17, 687–99.

Gottardi, G. and Galli, E. (1985) *Natural Zeolites*, Springer Verlag, Berlin Heidelberg, 409 pp.

——and Obradović, J. (1978) *Fortschr. Mineral.* **56,** 316–66.

Hawkins, D. B., Sheppard, R. A. and Gude, A. J., 3rd (1978) *Natural Zeolites: Occurrence, Properties, Use* (L. B. Sand and F. A. Mumpton, eds.) Pergamon Press, Elmsford, New York, 337–43.

Hay, R. L. (1966) *Geol. Soc. Am. Spec. Pap.* 85, 130 pp.

——and Guldman, S. G. (1987) *Clays Clay Minerals,* **35,** 449–57.

——and Sheppard, R. A. (1977) *Mineralogy and Geology of Natural Zeolites* (F. A. Mumpton, ed.) *Reviews in Mineralogy* **4,** Mineral Soc. Am., Washington, D.C., 93–102.

Hemley, J. (1962) Geol. Soc. Am. Abstracts for 1961. *Geol. Soc. Am. Spec. Pap.* 68, 196.

Iijima, A. (1978) *Natural Zeolites: Occurrence, Properties, Use* (L. B. Sand and F. A. Mumpton, eds.) Pergamon Press, Elmsford, New York, 175–98.

——and Utada, M. (1971) *Molecular Sieve Zeolites I,* Advances in Chemistry Series, 101 (R. F. Gould, ed.) Am. Chem. Soc., Washington, D.C., 342–9.

Kanazirski, M. M. and Yanev, Y. Ya. (1983) *C.R. Acad. Bulg. Sci.* **36,** 1571–4.

Lilov, P., Yanev, Y. and Marchev, P. (1987) *First Bulgarian–Greek Symposium, Smolyan, Abstracts,* 63.

Marantos, J., Kosiaris, G., Karantasis, S. and Grigoriades, G. (1988) *Study of the Tertiary zeolitic pyroclastic rocks of Metaxades, Evros county.* Unpublished report, Institute of Geology and Mineral Exploration, Athens, 12 pp. (in Greek).

Mason, B. and Sand, L. B. (1960) *Am. Mineral.* 45, 341–50.

Moncure, G. K.., Surdam, R. C. and Mckagne, H. L. (1981) *Clays Clay Minerals,* **29,** 385–96.

Mumpton, F. A. (1960) *Am. Mineral.* **45,** 351–69.

Petrov, O. E., Karamaneva, T. A. and Kirov, G. N. (1984) *C.R. Acad. Bulg. Sci.* **37,** 785–8.

Ratterman, N. G. and Surdam, R. C. (1981) *Clays Clay Minerals*, **29,** 365–77.

Shepard, A. O. (1961) Geological Survey Research. U.S. Geol. Surv. Prof. Pap. 424-C, C320–22.

Solakious, N. and Papadopoulos, P. (1988) *Micropalaeontological and Palaeographical evolution of the Oligocene, Thrace.* Unpublished report, Institute of Geology and Mineral exploration, Athens, 10 pp. (in Greek).

Tsirambides, A., Kassoli-Fournaraki, A., Filippidis, A. and Soldatos, K. (1988) *4th Congress of the Geological Society of Greece, Abstracts,* 110–11.

Tsolis-Katagas, P. and Katagas, C. (1989) *Clays Clay Minerals* (in press).

Utada, M. (1970) *Sci. Papers Coll. Gen. Educ. Univ. Tokyo,* **20,** 191–262.

[*Manuscript received 25 July 1989; revised 9 October 1989*]